Reduction of Cascading Outage Risk Based on Risk Gradient and Markovian Tree Search

Rui Yao, *Member, IEEE,* Kai Sun, *Senior Member, IEEE,* Feng Liu, *Member, IEEE,* Shengwei Mei, *Fellow, IEEE*

arXiv:1704.02556v1 [cs.SY] 9 Apr 2017

***Abstract*—Since cascading outages are major threats to power system operations, it is of great significance to reduce the risk of potential cascading outages. In this paper, a method for reduction of cascading outage risk based on Markovian tree (MT) search is proposed. Based on the MT expansion of the cascading outage risk, the risk gradient is computed with a forward-backward tree search scheme. The computation of risk gradient is incorporated into the procedure of risk assessment based on MT search, which is efficient with good convergence. Then the an optimization model for risk reduction (RR) is formulated by using risk gradient, which minimizes the cost of control while effectively reduces the cascading outage risk. Moreover, to overcome the limitation of linearization, an iterative risk reduction (IRR) algorithm is further developed. Test results on a 4-bus test system and the RTS-96 3-area test system verify the accuracy of risk gradient computation and effectiveness of the RR. And the performance of the IRR is demonstrated on RTS-96 3-area system and a 410-bus US-Canada northeast system model. The results show that the subsequent cascade risk and the total risk are reduced by 93.6% and 54.5%, respectively.**

***Index Terms*—cascading outage, tree search, risk reduction, risk gradient, control cost, multi-object optimization**

I. Introduction

CASCADING outages are major threats to power system operations. In recent years, even though people have learned lessons from blackouts caused by cascading outages, and various measures have been proposed for prevention and mitigation, cascading outages still occur from time to time [1]. The mitigation methods [2]–[4] based on power-law analysis can only provide rough mitigation strategies in the planning horizon, lacking accurate tactics for operations. For mitigation in operations, an extensively used approach is deterministic N-1 or N-k contingency analysis, which guarantees that no limit is violated under given outage sets. Another methodology is robust optimization [5], which ensures the strategy to cover all foreseen high-risk scenarios. However, the prevention of all potential cascading outages could be too expensive for both planning and operations of the system. Also it is practically infeasible to completely wipe out the risk of cascading outages [6]. Hence, these deterministic or robust methods have limitations in the prevention and mitigation of cascading outages, and risk-based methods are expected as promising alternatives.

This work was supported by the CURENT Engineering Research Center.

R. Yao and K. Sun are with the Department of EECS, University of Tennessee, Knoxville, TN 37996, USA (emails: yaorui.thu@gmail.com, kaisun@utk.edu).

F. Liu and S. Mei are with the State Key Laboratory of Power Systems, Department of Electrical Engineering, Tsinghua University, Beijing 100084, China. (email: lfeng@mail.tsinghua.edu.cn)

Risk-based approaches have been proposed in various time frames, e.g. long-term planning, short-term planning and operations. Some methods apply risk indices based on predefined severity functions to optimization models [7], [8]. But a severity-based risk index may not have clear physical meaning. Also some methods incorporate reliability indices into the economic dispatch or unit commitment models [9], and thus achieves coordinated optimization between the economic profit and operation risk [10]. However, these methods fail to consider the dependency among outages, which may underestimate the risk of cascading outages.

Reasonable simulation and efficient risk assessment are prerequisites for practical reduction of cascading outage risk [6], [11]. Our previous work [12] proposed a quasi-dynamic multi-timescale method for simulation of cascaidng outages, which focuses on interactions among processes of different timescales in propagation of outages. Then, [13] proposed a risk assessment method based on Markovian tree (MT) search, which effectively avoids simulation of duplicated outage paths and thus enhances efficiency. It should be noted that the risk assessment method derives the risk in an expansion form corresponding to the tree structure, which can be further analyzed and utilized in risk reduction if the relationship between the risk and the system control variables (e.g. generator outputs, load curtailment, etc.) can be quantified.

This paper proposes a risk gradient derived from the MT-based risk assessment result, and develops a risk reduction method by using the risk gradient. The risk is linearized with the chain rule of derivatives of system states. The gradient of risk in the space of control variables is calculated recursively on the MT. The algorithm is incorporated in the forward-backward tree search scheme of risk assessment, so the calculation of risk gradient is realized efficiently within the procedure of risk assessment. The risk reduction (RR) is realized by incorporating the risk gradient into routine optimization problems and solving the dispatch strategy, which reflects the coordination between risk and control cost. Moreover, to overcome the limitation of linearization, an iterative risk reduction (IRR) is further proposed that derives more practical reduction of cascading outage risk.

The proposed method advantages in four folds:

1) The proposed method is based on the modeling and risk assessment of multi-level dependent cascading outages, which is more suitable for the prevention and mitigation of cascading outages than the existing methods that only considers current state or independent outages.

2) The risk and cost in the proposed model have clear physical meaning (load or economy loss), which facilitates

practical decision support.

3) The risk gradient derived from the MT expansion of risk enables the incorporation of risk reduction into optimization models of dispatch, so the coordination between cost and risk can be efficiently achieved.

4) The forward-backward tree search algorithm as well as the good convergence of risk render promising computational efficiency for offline analysis and potential online support.

The rest of the paper is organized as follows. Section II briefly reviews the mechanism of risk assessment based on MT search, and then the generic form of risk mitigation using risk gradient is proposed. Section III proposes a forward-backward scheme for efficient calculation of risk gradient. Section IV realizes the RR model with the obtained risk gradient, and the IRR is presented to overcome the limitation of linearization. The cascading outage mitigation methods are verified on 4-bus, RTS-96 test systems and a US-Canada real-world system in Section V. Section VI is the conclusion.

II. Generic Model of Risk Reduction Based on MT and Risk Gradient

A. Retro of risk assessment using Markovian tree search

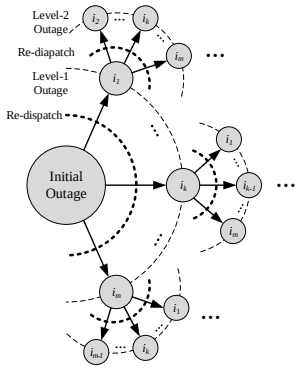

Fig. 1. MT representation of cascading outage paths

The risk mitigation needs quantified risk information. This paper is based on our previous work on efficient risk assessment method with Markovian tree search [13], and the quasi-dynamic simulation method [12]. All the possible cascading outage paths are organized in a MT, as shown in Fig. 1.

The time elapse is incorporated in the MT model, where each level on the MT corresponds to a time interval τ_D, and each node is labeled with the outage sequence from the root, as $(i_{k_1}\cdots i_{k_n})$, where i_{k_r} is either a positive integer denoting the index of the element failed on the rth level or 0 if no outage occurs on this level, n is the ending level of the cascading outage. The cost corresponding to state $(i_{k_1}\cdots i_{k_n})$ is $C(i_{k_1}\cdots i_{k_n})$, and the conditional probability of outage event $i_{k_{r+1}}$ after state $(i_{k_1}\cdots i_{k_r})$ is $\Pr(i_{k_{r+1}}|i_{k_1}\cdots i_{k_r})$. Then with the MT structure, the risk is expressed as the following expansion [13]:

$$
\begin{aligned}
R = {} & C_0 + \sum_{k_1}\Pr(i_{k_1})C(i_{k_1}) \\
& + \sum_{k_1}\Pr(i_{k_1})\sum_{k_2}\Pr(i_{k_2}|i_{k_1})C(i_{k_1}i_{k_2}) \\
& + \sum_{k_1}\Pr(i_{k_1})\sum_{k_2}\Pr(i_{k_2}|i_{k_1})\sum_{k_3}\Pr(i_{k_3}|i_{k_1}i_{k_2})C(i_{k_1}i_{k_2}i_{k_3}) \\
& + \cdots
\end{aligned}
\tag{1}
$$

Suppose a remedial action is taken to reduce the cascading outage risk right after initial outages. Then the expansion (1) can be divided into two parts: C_0 is the cost of the remedial action, and all the rest terms are risks of subsequent cascading outages, whose sum is denoted by R'. The risk is assessed by searching the MT and adding risk terms corresponding to newly-visited states in (1). The tree search scheme avoids duplicated simulation of cascading paths and significantly saves computation time.

To further accelerate the computation, a forward-backward tree search algorithm based on a risk estimation index (REI) was proposed, as is illustrated in Fig. 2.

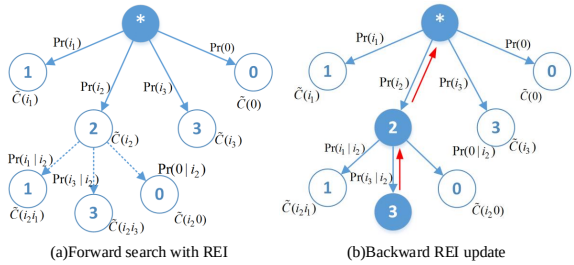

Fig. 2. Forward-backward search strategy in MT risk assessment

B. Generic optimization model of risk reduction

Cascading outages in the early stage usually develop slowly, so there is some time to adjust system states to reduce the risk of potential cascading outages after initial outage. A control action after the initial outage results in cost C_0 while reducing risk R', so a compromise between the effect and cost of risk reduction should be concerned. It is desirable that the risk of subsequent cascading outages is confined below a certain level R'_S, while the cost of control is minimized. Therefore, the basic formulation of risk reduction can be written as

$$
\begin{aligned}
& \min f = C_0(\mathbf{x}^*) \\
& s.t.\ R'(\mathbf{x}^*) \le R'_S \\
& \mathbf{g}(\mathbf{x}^*) \le \mathbf{0}
\end{aligned}
\tag{2}
$$

where $\mathbf{x}^*$ is the target system state, and $C_0(\mathbf{x}^*)$ is the cost of control, $R'(\mathbf{x}^*)$ is the subsequent risk. The last constraint contains the constraints in operations, e.g. load, generation and transmission capacity constraints. In this paper, $C_0(\mathbf{x}^*)$ is the objective of minimum redispatch in DC power flow model:

$$
C_0(\mathbf{x}^*) = -\mathbf{c}_D^{\mathrm{T}}(\mathbf{P}_d^* - \mathbf{P}_d) + \mathbf{c}_G^{\mathrm{T}}|\mathbf{P}_g^* - \mathbf{P}_g| \tag{3}
$$

Here $\mathbf{x}^* = [\mathbf{P}_d^{*\mathrm{T}}, \mathbf{P}_g^{*\mathrm{T}}]^{\mathrm{T}}$ is a vector of target re-dispatch state. $\mathbf{x} = [\mathbf{P}_d^{\mathrm{T}}, \mathbf{P}_g^{\mathrm{T}}]^{\mathrm{T}}$ is the pre-control system state. $\mathbf{c}_D$ and $\mathbf{c}_G$

are per MW costs of load shedding and generation adjustment, respectively.

However, quantifying R' as a function of $\mathbf{x}^*$ in (2) is not straightforward. Since cascading outages involve complex dependent events, any change in the system state will affect all following states, and thus the risk terms on all levels of the MT are changed. Therefore, it is infeasible to get analytical form of R' as a function of $\mathbf{x}^*$, but we can linearize the risk at the original target state $\mathbf{x}_0^*$, and obtain the risk gradient:

$$\mathbf{\Gamma} = \left.\frac{\partial R'}{\partial \mathbf{x}^*}\right|_{\mathbf{x}^*=\mathbf{x}_0^*} \tag{4}$$

then the risk reduction model (2) becomes

$$\begin{aligned} &\min f = C_0(\mathbf{x}^*) \\ &s.t.\ \mathbf{\Gamma}\cdot(\mathbf{x}^* - \mathbf{x}_0^*) \le R'_S - R'_0 \\ &\quad \mathbf{g}(\mathbf{x}^*) \le \mathbf{0} \end{aligned} \tag{5}$$

The next section will address calculation of the risk gradient by using the result of risk assessment.

III. Calculation of Risk Gradient

A. Derivative chain of states on the MT

From (1) and (5), the risk gradient depends on the derivatives of conditional probability $\Pr(i_{k_r}|i_{k_1}\cdots i_{k_{r-1}})$ and cost $C(i_{k_1}\cdots i_{k_r})$ of states on each level of the MT. Such calculation requires the analysis of the chain of states on the cascading outage path. As shown in Fig.3, denote the post-outage state on the rth level as $\mathbf{x}^{(r)\prime}$, and the state after re-dispatch as $\mathbf{x}^{(r)*}$. The costs of the short-timescale process and re-dispatch of all $i_{k_r}(r=1,\cdots,n)$ are briefly denoted as vectors $\mathbf{C}_F^{(r)}$ and $\mathbf{C}_R^{(r)}$, respectively, and the total cost on level r is $\mathbf{C}^{(r)} = \mathbf{C}_F^{(r)} + \mathbf{C}_R^{(r)}$. Denote outage probabilities as $\mathbf{Pr}^{(r)}$.

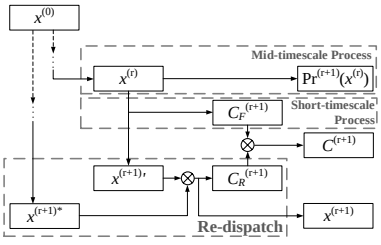

Fig. 3. State dependencies on one level of cascading outage

In this paper, we assume that the probabilities and the costs are differentialble. If in reality these quantities are non-smooth or discontinuous functions of states, then they need to be treated in segments or use the sub-derivatives as an approximation. And if there are discrete variables, then they need to be treated as continuous ones temporarily. To calculate the gradient of risk, the terms $\frac{\partial \mathbf{Pr}^{(r)}}{\partial \mathbf{x}^{(0)}}$ and $\frac{\partial \mathbf{C}^{(r)}}{\partial \mathbf{x}^{(0)}}$ are necessary according to (1). In fact, according to Fig.3, if the partial derivatives on each level up to r, i.e. $\frac{\partial \mathbf{C}^{(r)}}{\partial \mathbf{x}^{(r-1)}}$, $\frac{\partial \mathbf{Pr}^{(r)}}{\partial \mathbf{x}^{(r-1)}}$ and $\frac{\partial \mathbf{x}^{(r)}}{\partial \mathbf{x}^{(r-1)}}$ are obtained, then $\frac{\partial \mathbf{Pr}^{(r)}}{\partial \mathbf{x}^{(0)}}$ and $\frac{\partial \mathbf{C}^{(r)}}{\partial \mathbf{x}^{(0)}}$ can be calculated iteratively. The derivation of the partial derivatives on each level depends on the analysis of the cascading process, which will be elucidated below.

1) Mid-term Random Outage: The probability of element i outage on the MT is [13]:

$$\Pr_i^{\mathrm{MT}} = \frac{\lambda_i}{\sum_j \lambda_j}\left(1 - \mathrm{e}^{-\sum_j \lambda_j \tau_D}\right) \tag{6}$$

where λ_i is the failure rate of branch element i, and is assumed to be a function of its branch flow F_i [3], [14], [15]. And F_i is a function of system state $\mathbf{x}$. So the partial derivative of level $r+1$ branch outage probability with respect to state $\mathbf{x}^{(r)}$ is

$$\frac{\partial \mathbf{Pr}^{(r+1)}}{\partial \mathbf{x}^{(r)}} = \frac{\partial \mathbf{Pr}^{(r+1)}}{\partial \lambda}\cdot\frac{\partial \lambda}{\partial \mathbf{F}}\cdot\left[-\mathbf{y}_D\mathbf{M}\mathbf{Y}^+, \mathbf{y}_D\mathbf{M}\mathbf{Y}^+\right] \tag{7}$$

where λ and $\mathbf{F}$ are vectors of λ_i and F_i, respectively. $\mathbf{y}_D$ is a diagonal matrix of branch admittances. $\mathbf{M}$ is a $|V|\times|E|$ matrix and each of its column M_{i_k} corresponding to a branch $i_k = \{u, v\}$ satisfies $M_{i_k,u} = 1$, $M_{i_k,v} = -1$ and all the other entries are 0. $\mathbf{Y}^+$ is the Penrose-Moore pseudo-inverse of admittance matrix $\mathbf{Y}$.

2) Short-timescale process: As Fig. 4 shows, a short-timescale process may comprise of several outages, and each outage may directly lead to cost on loss of load due to load shedding [16]. The cost of short-timescale outages on level $r+1$ is the sum of costs caused by all outages.

$$\mathbf{C}_F^{(r+1)} = \sum_{k=1}^{n_{r+1}} \mathbf{C}_F^{(k|r+1)} \tag{8}$$

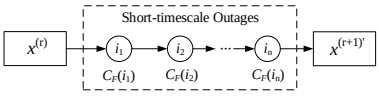

Fig. 4. Illustration of short-timescale outage events and costs

where n_{r+1} is the number of short-timescale outages on level $r+1$, and the cost of the kth outage is $\mathbf{C}_F^{(k|r+1)}$. $\mathbf{x}^{(k|r+1)}$ is the state after kth outage on level $r+1$, and each $\mathbf{x}^{(k|r+1)}$ is obtained from simulation (note that $\mathbf{x}^{(0|r+1)} = \mathbf{x}^{(r)}$ and $\mathbf{x}^{(n_{r+1}|r+1)} = \mathbf{x}^{(r+1)\prime}$). Also $\frac{\partial \mathbf{x}^{(k|r+1)}}{\partial \mathbf{x}^{(k-1|r+1)}}$ and $\frac{\partial \mathbf{C}_F^{(k|r+1)}}{\partial \mathbf{x}^{(k-1|r+1)}}$ can be derived by sensitivity analysis of load shedding [17], [18].

As simulation of each outage on level $r+1$ continues, $\frac{\partial \mathbf{x}^{(k|r+1)}}{\partial \mathbf{x}^{(r)}}$ can be derived with:

$$\frac{\partial \mathbf{x}^{(k|r+1)}}{\partial \mathbf{x}^{(r)}} = \frac{\partial \mathbf{x}^{(k|r+1)}}{\partial \mathbf{x}^{(k-1|r+1)}}\cdot\frac{\partial \mathbf{x}^{(k-1|r+1)}}{\partial \mathbf{x}^{(r)}} \tag{9}$$

$$\frac{\partial \mathbf{C}_F^{(k|r+1)}}{\partial \mathbf{x}^{(r)}} = \frac{\partial \mathbf{C}_F^{(k|r+1)}}{\partial \mathbf{x}^{(k-1|r+1)}}\cdot\frac{\partial \mathbf{x}^{(k-1|r+1)}}{\partial \mathbf{x}^{(r)}} \tag{10}$$

From Fig. 4, the partial derivative of states in short-timescale outages $\frac{\partial \mathbf{x}^{(r+1)\prime}}{\partial \mathbf{x}^{(r)}}$ is obtained by applying (9) iteratively. And from (8) and (10), the partial derivative of the short-timescale outage cost is derived as

$$\frac{\partial \mathbf{C}_F^{(r+1)}}{\partial \mathbf{x}^{(r)}} = \sum_{k=1}^{n_{r+1}} \frac{\partial \mathbf{C}_F^{(k|r+1)}}{\partial \mathbf{x}^{(r)}} \tag{11}$$

3) Re-dispatch: Re-dispatch is usually modeled as an optimization problem. In the DC power flow model, the execution of re-dispatch can be modeled as a linear programming (LP) problem, which can be briefly denoted as follows [13]:

$$\mathbf{x}^{(r+1)} = LP_e(\mathbf{p}^{(r+1)}, \mathbf{x}^{(r+1)\prime}, \mathbf{x}^{(r+1)*}, \tau_D) \tag{12}$$

where $\mathbf{p}^{(r+1)}$ is the parameters on the $r+1$th level, such as network topology, branch parameters, branch flow limit, etc. $\mathbf{x}^{(r+1)*}$ is the re-dispatch target state to fulfill, which is determined by another LP problem [13], [14] as:

$$\mathbf{x}^{(r+1)*} = LP_a(\mathbf{p}^{(r+1)}, \mathbf{x}^{(r+1)\prime}) \tag{13}$$

From (12), $\frac{\partial \mathbf{C}_R^{(r+1)}}{\partial \mathbf{x}^{(r+1)\prime}}$, $\frac{\partial \mathbf{C}_R^{(r+1)}}{\partial \mathbf{x}^{(r+1)*}}$, $\frac{\partial \mathbf{x}^{(r+1)}}{\partial \mathbf{x}^{(r+1)\prime}}$ and $\frac{\partial \mathbf{x}^{(r+1)}}{\partial \mathbf{x}^{(r+1)*}}$ can be obtained by means of Lagrange multiplier and sensitivity analysis [19]. Similarly, $\frac{\partial \mathbf{x}^{(r+1)*}}{\partial \mathbf{x}^{(r+1)\prime}}$ can be calculated from (13).

B. Iterative calculation of terms in risk gradient

With the analysis in III.A and chain rule of derivatives, the terms $\frac{\partial \mathbf{Pr}^{(r)}}{\partial \mathbf{x}^{(0)}}$ and $\frac{\partial \mathbf{C}^{(r)}}{\partial \mathbf{x}^{(0)}}$ of each level r can be calculated. Assume for any level m ($1 \le m \le r$), terms $\frac{\partial \mathbf{x}^{(m)}}{\partial \mathbf{x}^{(0)}}$, $\frac{\partial \mathbf{x}^{(m)\prime}}{\partial \mathbf{x}^{(0)}}$ and $\frac{\partial \mathbf{x}^{(m)*}}{\partial \mathbf{x}^{(0)}}$ are obtained, then for level $r+1$ the terms $\frac{\partial \mathbf{x}^{(r+1)}}{\partial \mathbf{x}^{(0)}}$, $\frac{\partial \mathbf{x}^{(r+1)\prime}}{\partial \mathbf{x}^{(0)}}$ and $\frac{\partial \mathbf{x}^{(r+1)*}}{\partial \mathbf{x}^{(0)}}$ are obtained as follows

$$\frac{\partial \mathbf{x}^{(r+1)\prime}}{\partial \mathbf{x}^{(0)}} = \frac{\partial \mathbf{x}^{(r+1)\prime}}{\partial \mathbf{x}^{(r)}} \cdot \frac{\partial \mathbf{x}^{(r)}}{\partial \mathbf{x}^{(0)}} \tag{14}$$

$$\frac{\partial \mathbf{x}^{(r+1)*}}{\partial \mathbf{x}^{(0)}} = \frac{\partial \mathbf{x}^{(r+1)*}}{\partial \mathbf{x}^{(r+1)\prime}} \cdot \frac{\partial \mathbf{x}^{(r+1)\prime}}{\partial \mathbf{x}^{(0)}} \tag{15}$$

$$\frac{\partial \mathbf{x}^{(r+1)}}{\partial \mathbf{x}^{(0)}} = \frac{\partial \mathbf{x}^{(r+1)}}{\partial \mathbf{x}^{(r+1)*}} \cdot \frac{\partial \mathbf{x}^{(r+1)*}}{\partial \mathbf{x}^{(0)}} + \frac{\partial \mathbf{x}^{(r+1)}}{\partial \mathbf{x}^{(r+1)\prime}} \cdot \frac{\partial \mathbf{x}^{(r+1)\prime}}{\partial \mathbf{x}^{(0)}} \tag{16}$$

Since $\frac{\partial \mathbf{x}^{(1)*}}{\partial \mathbf{x}^{(0)}}$, $\frac{\partial \mathbf{x}^{(1)\prime}}{\partial \mathbf{x}^{(0)}}$ and $\frac{\partial \mathbf{x}^{(1)}}{\partial \mathbf{x}^{(0)}}$ can be obtained from III.A, so according to (14)-(16), for any r ($1 \le r \le n$, where n is the final level of cascading outage), $\frac{\partial \mathbf{x}^{(r)*}}{\partial \mathbf{x}^{(0)}}$, $\frac{\partial \mathbf{x}^{(r)\prime}}{\partial \mathbf{x}^{(0)}}$ and $\frac{\partial \mathbf{x}^{(r)}}{\partial \mathbf{x}^{(0)}}$ are obtained iteratively in the process of cascading outage path simulation. So $\frac{\partial \mathbf{Pr}^{(r)}}{\partial \mathbf{x}^{(0)}}$ and $\frac{\partial \mathbf{C}^{(r)}}{\partial \mathbf{x}^{(0)}}$ are calculated with

$$\frac{\partial \mathbf{Pr}^{(r)}}{\partial \mathbf{x}^{(0)}} = \frac{\partial \mathbf{Pr}^{(r)}}{\partial \mathbf{x}^{(r-1)}} \cdot \frac{\partial \mathbf{x}^{(r-1)}}{\partial \mathbf{x}^{(0)}} \tag{17}$$

$$\begin{aligned}\frac{\partial \mathbf{C}^{(r)}}{\partial \mathbf{x}^{(0)}} =& \frac{\partial \mathbf{C}_F^{(r)}}{\partial \mathbf{x}^{(r-1)}} \cdot \frac{\partial \mathbf{x}^{(r-1)}}{\partial \mathbf{x}^{(0)}} + \\ & \frac{\partial \mathbf{C}_R^{(r)}}{\partial \mathbf{x}^{(r-1)\prime}} \cdot \frac{\partial \mathbf{x}^{(r-1)\prime}}{\partial \mathbf{x}^{(0)}} + \frac{\partial \mathbf{C}_R^{(r)}}{\partial \mathbf{x}^{(r-1)*}} \cdot \frac{\partial \mathbf{x}^{(r-1)*}}{\partial \mathbf{x}^{(0)}}\end{aligned} \tag{18}$$

C. Recursive form of risk gradient

Define equivalent cascading outage cost $C'(i_{k_1} \cdots i_{k_r})$ as

$$\begin{aligned}&C'(i_{k_1} \cdots i_{k_r}) \triangleq C(i_{k_1} \cdots i_{k_r}) + \\ &\sum_{i_{k_{r+1}}} \Pr(i_{k_{r+1}} | i_{k_1} \cdots i_{k_r}) C(i_{k_1} \cdots i_{k_{r+1}}) + \cdots \\ &= C(i_{k_1} \cdots i_{k_r}) + \sum_{i_{k_{r+1}}} \Pr(i_{k_{r+1}} | i_{k_1} \cdots i_{k_r}) C'(i_{k_1} \cdots i_{k_{r+1}})\end{aligned} \tag{19}$$

(19) shows a recursive relationship, so $C'(i_{k_1} \cdots i_{k_r})$ could be calculated and updated reversely from the terminal back to the root of the MT. Similarly, define

$$R'(i_{k_1} \cdots i_{k_{r+1}}) \triangleq \sum_{i_{k_{r+1}}} \Pr(i_{k_{r+1}} | i_{k_1} \cdots i_{k_r}) C'(i_{k_1} \cdots i_{k_{r+1}}) \tag{20}$$

With given $i_{k_1} \cdots i_{k_r}$, abbreviate all $R'(i_{k_1} \cdots i_{k_{r+1}})$ as vector $\mathbf{R}^{(r)\prime}$, and $C'(i_{k_1} \cdots i_{k_r})$ as $\mathbf{C}^{(r)\prime}$, then

$$\frac{\partial R'(i_{k_1} \cdots i_{k_r})}{\partial \mathbf{x}^{(0)}} = \mathbf{C}^{(r)\prime\,\mathrm{T}} \frac{\partial \mathbf{Pr}^{(r)}}{\partial \mathbf{x}^{(0)}} + \mathbf{Pr}^{(r)\,\mathrm{T}} \left(\frac{\partial \mathbf{C}^{(r)}}{\partial \mathbf{x}^{(0)}} + \frac{\partial \mathbf{R}^{(r)\prime}}{\partial \mathbf{x}^{(0)}} \right) \tag{21}$$

(21) is also a recursive form. Note that $R^{(0)\prime} = R'$, so the gradient of risk can be computed with forward-backward scheme in the risk assessment based on MT search.

D. Forward-backward scheme of risk gradient calculation

With (14)-(18), the partial derivatives are calculated in the process of forward searching with the MT-search based risk assessment [13], as demonstrated in Algorithm 1.

Algorithm 1. Forward calculation of partial derivatives

Step 1. Initialize level on MT $r = 0$.
Step 2. Sample mid-timescale outages and calculate $\frac{\partial \mathbf{Pr}^{(r+1)}}{\partial \mathbf{x}^{(r)}}$ with (7).
Step 3. Simulate short-timescale outages, and calculate $\frac{\partial \mathbf{x}^{(r+1)\prime}}{\partial \mathbf{x}^{(r)}}$, $\frac{\partial \mathbf{C}_F^{(r+1)}}{\partial \mathbf{x}^{(r)}}$ with (8)-(11).
Step 4. Simulate re-dispatch. Calculate $\frac{\partial \mathbf{Pr}^{(r+1)}}{\partial \mathbf{x}^{(0)}}$, $\frac{\partial \mathbf{x}^{(r+1)}}{\partial \mathbf{x}^{(0)}}$ and $\frac{\partial \mathbf{C}^{(r+1)}}{\partial \mathbf{x}^{(0)}}$.
Step 5. If the cascading outage path ends, exit and start simulation of a new path. Otherwise assign $r = r+1$ and jump to Step 2.

After searching a cascading outage path on the MT, the risk gradient is updated reversely, as Algorithm 2 shows.

Algorithm 2. Backward update of risk gradient.

Assume the cascade path is $i_{k_1} \cdots i_{k_n}$, the variables with superscript (r) correspond to $(i_{k_1} \cdots i_{k_r})$, and (0) correspond to the root state on MT.

Step 1. Define $b^{(r)}, r = 1 \cdots n$. If state $(i_{k_1} \cdots i_{k_r})$ has been reached before, then $b^{(r)} = 0$, otherwise $b^{(r)} = 1$.
Step 2. Assign $r = n$. Assign $\mathbf{S}^{(r)} = b^{(r)} \frac{\partial C^{(r)}}{\partial \mathbf{x}^{(0)}}$, $\Delta C^{(r)} = b^{(r)} \cdot C^{(r)}$.
Step 3. Reverse to the previous state on the cascade path. Assign $r = r-1$.
Step 4. Let $\mathbf{S}^{(r)} = \mathrm{Pr}^{(r+1)} \mathbf{S}^{(r+1)} + \Delta C^{(r+1)} \frac{\partial \mathrm{Pr}^{(r+1)}}{\partial \mathbf{x}^{(0)}}$.
Step 5. Let $\Delta C^{(r)} = b^{(r)} C^{(r)} + b^{(r+1)} \mathrm{Pr}^{(r+1)} \Delta C^{(r+1)}$.
Step 6. If $r = 0$ then exit. Otherwise jump to Step 3.

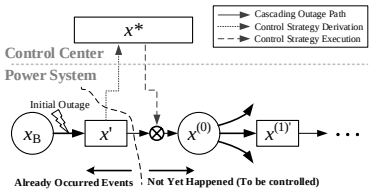

Fig. 5. Time series of the derivation and execution of control strategy

By applying Algorithms 1 and 2 repeatedly along with the forward searching and backward updating procedure of risk assessment [13], the $\mathbf{S}^{(0)}$ will converge to $\frac{\partial R^{(0)\prime}}{\partial \mathbf{x}^{(0)}}$. Note that in

operations, $\mathbf{x}^{(0)}$ is indirectly changed by altering the dispatch target state $\mathbf{x}^*$, as Fig. 5 shows. The gradient of risk is

$$\mathbf{\Gamma} = \mathbf{S}^{(0)} \cdot \frac{\partial \mathbf{x}^{(0)}}{\partial \mathbf{x}^*} \tag{22}$$

IV. Risk Reduction

A. Full optimization model of risk reduction (RR)

After the risk gradient is obtained in the space of control variables, the risk reduction (RR) optimization model is established based on the generic form of (5) as

$$\begin{aligned} &\min f = -\mathbf{c}_D^{\mathrm{T}} \left(\mathbf{P}_d^* - \mathbf{P}_d\right) + \mathbf{c}_G^{\mathrm{T}} \left|\mathbf{P}_g^* - \mathbf{P}_g\right| \\ &s.t. \\ &-\mathbf{\Gamma} \cdot \begin{bmatrix} \mathbf{P}_d^* - \mathbf{P}_{d0}^* \\ \mathbf{P}_g^* - \mathbf{P}_{g0}^* \end{bmatrix} \le R_E - R'(\mathbf{x}_0^{(0)*}) \\ &\mathbf{1}^{\mathrm{T}} \left(\mathbf{P}_g^* - \mathbf{P}_d^*\right) = 0 \\ &-\mathbf{F}^{\max} \le \mathbf{y}_D \mathbf{M} \mathbf{Y}^{+} \left(\mathbf{P}_g^* - \mathbf{P}_d^*\right) \le \mathbf{F}^{\max} \\ &\mathbf{P}_g^{\min} \le \mathbf{P}_g^* \le \mathbf{P}_g^{\max} \\ &\mathbf{0} \le \mathbf{P}_d^* \le \mathbf{P}_d \end{aligned} \tag{23}$$

where the first constraint is the risk constraint based on risk gradient. $\mathbf{x}_0^{(0)*} = [\mathbf{P}_{d0}^{*\,\mathrm{T}}, \mathbf{P}_{g0}^{*\,\mathrm{T}}]^{\mathrm{T}}$ denote the target state of original working condition (from original dispatch strategy), $R'(\mathbf{x}_0^{(0)*})$ is the risk of subsequent cascades of original dispatch strategy, and R_E is the expected risk after mitigation. The other constraints are the limits of branches, generators and loads. Here the variables are continuous, so the RR is an LP problem. If there are discrete variables, then RR will become mixed-integer linear programming (MILP) problem.

The (23) reduces cascading outages risk by setting its solution as the target state of re-dispatch. The extent of risk reduction is adjusted by changing the expected subsequent cascade risk R_E. The constraint will force the solution to a less risky state and the control cost is expected to be higher. Denote the expected risk decrease as $\Delta R = R'(\mathbf{x}_0^{(0)*}) - R_E \ge 0$, the bigger ΔR, the more reduction of risk is expected.

B. Iterative risk reduction (IRR)

The RR model is based on the linearization of risk at the original operating point. When ΔR goes outside an effective region of linearization, then there will be considerable linearization errors. To overcome such limitation, consider iterating the procedure of RR so as to accumulate the effect of linearization-based RR step by step. The procedure of iterative RR (IRR) is shown as Fig. 6.

The IRR first assesses risk on original operating condition, and solves the RR problem (23). The new dispatch strategy is then evaluated with risk assessment. If the risk is decreased, then the strategy is expected to be effective. Such procedure is iterated until the risk does not decrease.

C. Framework of RR/IRR application

The RR and IRR can be used offline to generate mitigation strategy on pre-selected contingencies and system working conditions. The generated strategies are stored in database and can be extracted when corresponding contingencies occur. Moreover, the RR and IRR also have potential of online assessment and decision support. The framework of RR/IRR application is demonstrated in Fig. 7.

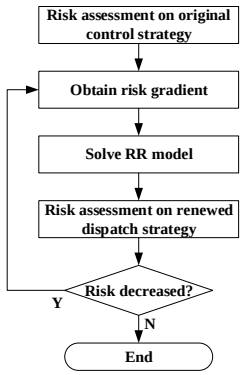

Fig. 6. The procedure of IRR

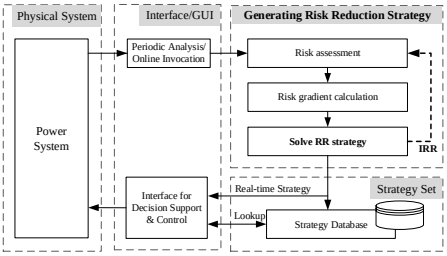

Fig. 7. The framework of RR/IRR application

V. Case Studies

A. Verification of risk gradient calculation in 4-bus system

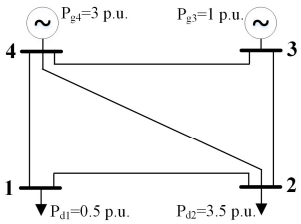

Fig. 8. 4-bus test system

First test the derivation of risk gradient in a 4-bus system. The system has 2 generation buses and 2 load buses, as shown in Fig. 8. Select the maximum duration of cascading outage simulation $T_{\max} = 60\text{min}$, and $\tau_D = 15\text{min}$. The state in injection space is denoted as $\mathbf{x} = [P_{d1}, P_{d2}, P_{g3}, P_{g4}]^{\mathrm{T}}$, and the dispatch target state is $\mathbf{x}^* = [P_{d1}^*, P_{d2}^*, P_{g3}^*, P_{g4}^*]^{\mathrm{T}}$. The $\frac{\partial \mathbf{x}^{(0)}}{\partial \mathbf{x}^*}$ at original condition is

$$\frac{\partial \mathbf{x}^{(0)}}{\partial \mathbf{x}^*} = \begin{bmatrix} 1 & 0 & 0 & 0 \\ 0 & 1 & 0 & 0 \\ 0 & 0 & 0 & 0 \\ 1 & 1 & 0 & 0 \end{bmatrix} \tag{24}$$

so $\frac{\partial \mathbf{x}^{(0)}}{\partial P^*_{g3}} = \mathbf{0}$, $\frac{\partial \mathbf{x}^{(0)}}{\partial P^*_{g4}} = \mathbf{0}$, changing P^*_{g3} and P^*_{g4} does not affect the risk. Therefore we can study the effect of changing P^*_{d1}, P^*_{d2}, and adjusting P^*_{g3} and P^*_{g4} accordingly to maintain the power balance. We estimate the risk gradient by making small disturbances to $\mathbf{x}^*$ and assess the changes in risk. In the original operating condition, $\mathbf{x}^* = [0.50, 2.54, 1.00, 2.04]^{\mathrm{T}}(\mathrm{p.u.})$. Assume the magnitude of disturbance $\Delta P_N = 0.001\mathrm{p.u}$, and set load disturbances $\Delta P^*_{d1} = \Delta P_N \sin\theta$,$\Delta P^*_{d2} = \Delta P_N \cos\theta$, where ancillary variable $\theta \in [0, 2\pi)$. This set of disturbances covers all possible directions on $\Delta P^*_{d1} - \Delta P^*_{d2}$ plane. Set $\Delta P^*_{g4} = 0$ and let P^*_{g3} change to balance the load change, i.e. $\Delta P^*_{g3} = \Delta P^*_{d1} + \Delta P^*_{d2}$. Choose 200 different values of θ evenly distributed in $[0, 2\pi)$, get 200 disturbances $\Delta \mathbf{x}^* = [\Delta P^*_{d1}, \Delta P^*_{d2}, \Delta P^*_{g3}, \Delta P^*_{g4}]^{\mathrm{T}}$, and calculate the changes of risk $\Delta R'$ with risk assessment, as shown in Fig. 9. Denote the risk gradient as $\mathbf{\Gamma} = [\gamma_{d1}, \gamma_{d2}, \gamma_{g3}, \gamma_{g4}]$, as $\gamma_{g3} = 0$, $\gamma_{g4} = 0$, so

$$\Delta R' = \gamma_{d1}\Delta P^*_{d1} + \gamma_{d2}\Delta P^*_{d2} \tag{25}$$

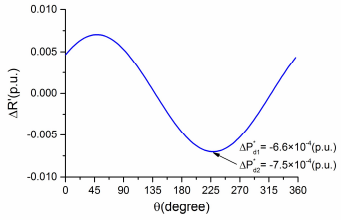

Fig. 9. Variation of risk under small disturbance of control strategy

With the 200 sets of ΔP^*_{d1}, ΔP^*_{d2} and $\Delta R'$, γ_{d1} and γ_{d2} can be estimated from (25) through linear regression. Here the estimation is $\hat{\gamma}_{d1} = 4.6482$, $\hat{\gamma}_{d2} = 5.2795$. Regression coefficient $\rho = 0.9999997$, showing very high credibility of the linear form (25). Therefore the estimated risk gradient is

$$\hat{\mathbf{\Gamma}} = [4.6482, 5.2795, 0, 0] \tag{26}$$

The risk gradient obtained with the proposed method is

$$\mathbf{\Gamma} = [4.6093, 5.2686, 0, 0] \tag{27}$$

$\mathbf{\Gamma}$ is very close to $\hat{\mathbf{\Gamma}}$, which verifies the accuracy of risk gradient calculation.

B. Convergence of risk gradient calculation in RTS-96 system

According to III.C, the calculation of risk gradient can be integrated into the forward-backward scheme of risk assessment. To efficiently derive risk mitigation strategy, the convergence of risk gradient is of great significance.

In the computation process, the risk gradient after the mth search attempt is denoted as $\mathbf{\Gamma}_m$, and the converged risk gradient is $\mathbf{\Gamma}^*$ on the MT. To evaluate the convergence profile of risk gradient, propose the following convergence indices:

$$\delta_m = \frac{\|\mathbf{\Gamma}_m - \mathbf{\Gamma}^*\|}{\|\mathbf{\Gamma}_1 - \mathbf{\Gamma}^*\|} \tag{28}$$

$$\delta^{\mathrm{dir}}_m = \left\| \frac{\mathbf{\Gamma}_m}{\|\mathbf{\Gamma}_m\|} - \frac{\mathbf{\Gamma}^*}{\|\mathbf{\Gamma}^*\|} \right\| \tag{29}$$

δ_m reflects the convergence of the vector of risk gradient, and δ^{dir}_m evaluates the convergence of the direction of risk gradient. We test on RTS-96 3-area system, the parameters are set as $T_{\max} = 150\mathrm{min}$, $\tau_D = 15\mathrm{min}$. After 10000 times of tree search, the risk, δ_m and δ^{dir}_m are all considered as converged. Fig. 10 and 11 demonstrate the convergence profile of risk gradient in the process of computation. The

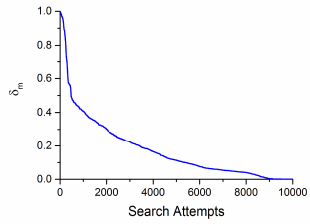

Fig. 10. Convergence of risk gradient

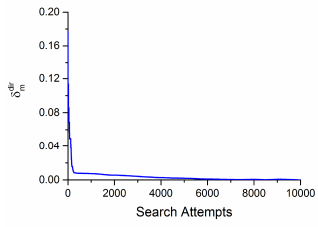

Fig. 11. Convergence of the direction of risk gradient

convergence of risk gradient is slower than that of risk [13] (as shown in Fig. 12). This is caused by the more complicated form of risk gradient, so the derivation of risk gradient may cost more computation time than risk assessment. However, the convergence of the direction of risk gradient only requires several hundreds of search attempts, which is much faster than the convergence of the vector of risk gradient. Actually, only obtaining the direction of risk gradient is enough for the reduction of risk, so in situations that require fast computation, the number of tree search attempts can be significantly reduced. However, in such a case, the accuracy of estimating the extent of risk reduction will be lower.

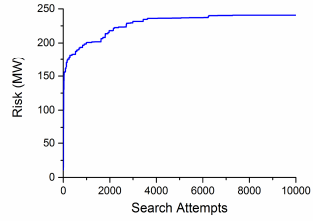

Fig. 12. Convergence profile of risk

C. Effectiveness of RR in RTS-96 test system

After validating the accuracy and convergence of the calculation of risk gradient, we test the effectiveness of RR in mitigating cascading outage risk in RTS-96 3-area test system.

Here we convert all the cost and risk into economic metrics. Assume that adjusting 1MW of generation in an interval τ_D costs 100 (e.g. dollars per hour), and 1MW load loss in an interval corresponds to loss of 10000. Set the initial failure on branches 22, 23 and 24. When utilizing conventional re-dispatch, the total risk (i.e. the cost of control plus the risk of subsequent cascading outages) is 696775. Then use RR to mitigate cascading outage risk and evaluate the performance with risk assessment. The effect of RR under different values of ΔR is shown in Fig. 13. The solid line is the risk after RR evaluated by risk assessment, while the dashed line is the expected risk. It can be seen that the RR effectively decreases risk within a certain range of ΔR. But the risk stops decreasing when ΔR reaches around 600000, which means the linearization is no longer effective.

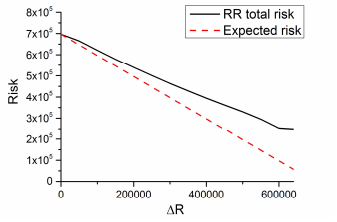

Fig. 13. Convergence profile of risk under RR

Next we compare the performance of RR with conventional severity-based methods in cascading outage mitigation. The risk-based OPF method (RB-OPF) [7] is tested in this case. In the RB-OPF, the risk can be reduced by lowering the upper limit of severity-based risk index $Risk_{\max}$. Decreasing $Risk_{\max}$ is expected to reduce the risk. Fig. 14 compares the costs of control and subsequent cascading outage risks under the RR and RB-OPF. It can be seen that RR achieves a lower risk than the RB-OPF at the same level of cost, so the RR is more effective in reducing the cascading outage risk.

Fig. 15 further annotates the cost-risk relationship with different values of $Risk_{\max}$ in the RB-OPF. The result shows that the relationship between cascading outage risk and $Risk_{\max}$ is non-smooth, which will cause difficulties in managing the cascading outage risk. By comparison, the RR proposed in this paper achieves a better performance in reducing risk, and the amount of risk reduction is more controllable.

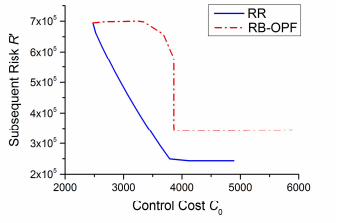

Fig. 14. Risk reduction performance of RR and RB-OPF

D. Coordination mitigation realized by IRR

1) RTS-96 System: The performance of the RR is limited only within a range where linearization is effective. Fig. 13 shows that with the RR, the risk stops decreasing at around 2.5×10^5. While the IRR can keep renewing risk gradient at updated operating points, so the risk can be further reduced. Table I and Fig. 16 demonstrates the cost-risk relationship at different rounds of iteration.

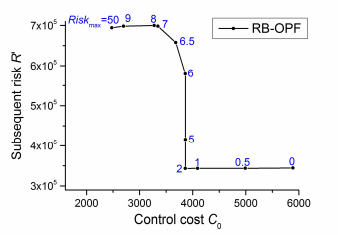

Fig. 15. Cost-risk characteristics under the RB-OPF

TABLE I
COST-RISK IN THE ITERATION PROCESS IN RTS-96 TEST SYSTEM

Round	ΔR	Control cost	Subsequent risk	Total risk
0	–	2475	694300	696775
1	600000	3789.8	249590	253379.8
2	100000	4141.6	174840	178981.6
3	100000	5034.9	40738	45772.9
4	20000	5456.4	12434	17890.4
5	1000	5590	13132	18722

The results indicate that the IRR can effectively overcome the limitation of linearization with the RR and further reduce risk of cascading outages. After 4 rounds of iterations, the subsequent risk of cascading outages has reduced by 97.3%.

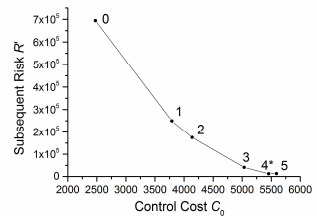

Fig. 16. Cost-risk trajectory of IRR in RTS-96 test system

2) US-Canada Northeast system: Next, the IRR is tested on a real-world system model, i.e. the simplified US-Canada Northeast power grid model [12] retaining all generator buses and the buses at 230 kV or above. The system contains 410 buses (287 load buses and 233 generator buses) and 882 branches. In this case, increase the system load to 1.5 times of the base load and set initial outages on branches 320 and 321. Utilize IRR to reduce the risk. The cost-risk characteristics with iterations of IRR are demonstrated in Fig. 17.

The results indicate that the total risk at the 6th iteration reaches the lowest among all iterations, where the total risk is expected to decrease by 54.5%, and the subsequent cascade risk drops significantly by 93.6%. The subsequent cascade risk is even lower in the 7th iteration, but the drop in subsequent cascade risk is offset by a substantially high cost, which causes a higher total risk than that of the 6th iteration. In practice,

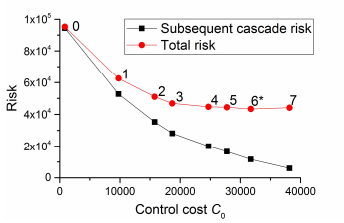

Fig. 17. Cost-risk trajectory of IRR in US-Canada Northeast system

the adopted strategy for risk reduction may vary depending on the risk preference. Therefore, the strategies in Fig. 17 can also be regarded as results of risk-cost multi-objective optimization, and the control strategy for risk reduction can be selected depending on risk preference.

As for the computational efficiency, the proposed method is developed with MATLAB and tested on a PC with 2.6GHz CPU and 32GB RAM. The average performance of a single IRR run in the US-Canada Northeast system model is shown in Table II. The result shows that solving the RR models takes only several seconds, but much more time is consumed in cascading outage simulation, risk assessment and calculating risk gradient. The speed of computation can be further enhanced with parallel computing on high-performance computation platform, and this method has potentials for online application on a 5-15 minute period for operators' decision support to prevent cascading outages.

TABLE II
TIME CONSUMPTION OF IRR IN US-CANADA NORTHEAST SYSTEM

Subprograms of IRR	**Time consumption (s)**
Cascading outage simulation & risk assessment	660.41
Computation of risk gradient	237.4
Solving RR model	3.48
Total	**901.31**

VI. CONCLUSION

This paper proposes a method for reducing the risk of cascading outages based on risk gradient and MT search. The expansion of risk is linearized in the space of control variables and then the gradient of risk is obtained. The computation of risk gradient adopts an efficient forward-backward algorithm, which can be combined with the procedure of risk assessment based on Markovian tree search, and the risk gradient has good convergence profile. With the risk gradient, the constraint of risk is established and incorporated into a dispatch model to formulate the risk reduction (RR) optimization model. The RR minimizes control cost while limiting the cascading outage risk under a preset level for a desirable compromise between cost and risk. The risk and cost in the RR model have clear physical meanings and thus can practically give insights for operators' decision support. The accuracy and efficiency of the RR are demonstrated and verified with a 4-bus test system and the RTS-96 test system.

To overcome the limitation of linearization in the RR, the iterative RR (IRR) is proposed to achieve effective reduction of cascading outages risk. The test case on US-Canada Northeast system model verifies that the IRR effectively reduces the subsequent cascading outage risk by 93.6% and the total risk by 54.5%. The RR and IRR may be utilized in online decision support for preventive control against potential cascading outages following possible contingency scenarios.

REFERENCES

[1] P. Hines, J. Apt, and S. Talukdar, "Large blackouts in north america: Historical trends and policy implications," *Energy Policy*, vol. 37, no. 12, pp. 5249–5259, 2009.

[2] B. A. Carreras, V. E. Lynch, D. E. Newman, and I. Dobson, "Blackout mitigation assessment in power transmission systems," in *Proceedings of the 36th Annual Hawaii International Conference on System Sciences*. IEEE, 2003, pp. 10–pp.

[3] J. Chen, J. S. Thorp, and I. Dobson, "Cascading dynamics and mitigation assessment in power system disturbances via a hidden failure model," *International Journal of Electrical Power & Energy Systems*, vol. 27, no. 4, pp. 318–326, 2005.

[4] D. E. Newman, B. A. Carreras, V. E. Lynch, and I. Dobson, "Exploring complex systems aspects of blackout risk and mitigation," *IEEE Trans. Reliab.*, vol. 60, no. 1, pp. 134–143, 2011.

[5] D. Bertsimas, E. Litvinov, X. A. Sun, J. Zhao, and T. Zheng, "Adaptive robust optimization for the security constrained unit commitment problem," *IEEE Trans. Power Syst.*, vol. 28, no. 1, pp. 52–63, 2013.

[6] M. Vaiman, K. Bell, Y. Chen, B. Chowdhury, I. Dobson, P. Hines, M. Papic, S. Miller, and P. Zhang, "Risk assessment of cascading outages: Methodologies and challenges," *IEEE Trans. Power Syst.*, vol. 27, no. 2, pp. 631–641, 2012.

[7] F. Xiao, *Risk based multi-objective security control and congestion management*. ProQuest, 2007.

[8] Q. Wang, J. D. McCalley, T. Zheng, and E. Litvinov, "A computational strategy to solve preventive risk-based security-constrained opf," *IEEE Trans. Power Syst.*, vol. 28, no. 2, pp. 1666–1675, 2013.

[9] D. N. Simopoulos, S. D. Kavatza, and C. D. Vournas, "Reliability constrained unit commitment using simulated annealing," *IEEE Trans. Power Syst.*, vol. 21, no. 4, pp. 1699–1706, 2006.

[10] J. He, L. Cheng, D. S. Kirschen, and Y. Sun, "Optimising the balance between security and economy on a probabilistic basis," *IET Generation, Transmission & Distribution*, vol. 4, no. 12, pp. 1275–1287, 2010.

[11] R. Yao, X. Zhang, S. Huang, S. Mei, Z. Zhang, X. Li, and Q. Zhu, "Cascading outage preventive control for large-scale ac-dc interconnected power grid," in *IEEE PES General Meeting*. IEEE, 2014, pp. 1–5.

[12] R. Yao, S. Huang, K. Sun, F. Liu, X. Zhang, and S. Mei, "A multi-timescale quasi-dynamic model for simulation of cascading outages," *IEEE Trans. Power Syst.*, vol. 31, no. 4, pp. 3189–3201, July 2016.

[13] R. Yao, S. Huang, K. Sun, F. Liu, X. Zhang, S. Mei, W. Wei, and L. Ding, "Risk assessment of multi-timescale cascading outages based on markovian tree search," *IEEE Trans. Power Syst.*, 2016.

[14] I. Dobson, B. A. Carreras, V. E. Lynch, and D. E. Newman, "An initial model for complex dynamics in electric power system blackouts," in *Proceedings of the Annual Hawaii International Conference on System Sciences*. Citeseer, 2001, pp. 51–51.

[15] M. Yang, J. Wang, H. Diao, J. Qi, and X. Han, "Interval estimation for conditional failure rates of transmission lines with limited samples," *IEEE Trans. Smart Grid*, 2016.

[16] H. Ren, I. Dobson, and B. A. Carreras, "Long-term effect of the n-1 criterion on cascading line outages in an evolving power transmission grid," *IEEE Trans. Power Syst.*, vol. 23, no. 3, pp. 1217–1225, 2008.

[17] C. Reddy, S. Chakrabarti, and S. Srivastava, "A sensitivity-based method for under-frequency load-shedding," *IEEE Trans. Power Syst.*, vol. 29, no. 2, pp. 984–985, 2014.

[18] A. A. Girgis and S. Mathure, "Application of active power sensitivity to frequency and voltage variations on load shedding," *Electric Power Systems Research*, vol. 80, no. 3, pp. 306–310, 2010.

[19] P. R. Gribik, D. Shirmohammadi, S. Hao, and C. L. Thomas, "Optimal power flow sensitivity analysis," *IEEE Trans. Power Syst.*, vol. 5, no. 3, pp. 969–976, 1990.